Paula Messina[1*]
Gerardo Prieto[1]
Verónica Dodero[2]
M. A. Cabrerizo-Vílchez[3]
J. Maldonado-Valderrama[3]
Juan M. Ruso[1]
Félix Sarmiento[1]

[1] *Grupo de Biofísica e Interfases, Departamento de Física Aplicada, Facultad de Física, Universidad de Santiago de Compostela, 15782 Santiago de Compostela, Spain*

[2] *Departamento de Química Orgánica, Facultad de Química, Universidad de Santiago de Compostela, 15782 Santiago de Compostela, Spain*

[3] *Grupo de Física de Fluidos y Biocoloides, Departamento de Física Aplicada, Facultad de Ciencias, Universidad de Granada, 18071 Granada, Spain*

Surface Characterization of Human Serum Albumin and Sodium Perfluorooctanoate Mixed Solutions by Pendant Drop Tensiometry and Circular Dichroism

Received 21 November 2005; revised 13 February 2006; accepted 21 February 2006

Published online 27 February 2006 in Wiley InterScience (www.interscience.wiley.com). DOI 10.1002/bip.20494

Abstract: *The interfacial behavior of mixed human serum albumin (HSA)/sodium perfluorooctanoate (C8FONa) solutions is examined by using two experimental techniques, pendant drop tensiometry and circular dichroism spectroscopy. Through the analysis of the surface tension of the mixed solutions, surface competitive adsorption at the air–water interface between C8FONa and HSA is detected. The dynamic adsorption curves exhibit the distinct regimes in their time-dependent surface tension. The nature of these regimes is further analyzed in terms of the variation of the molecules surface areas. As a consequence, a compact and dense structure was formed where protein molecules were interconnected and overlapped. Thus, a reduction of the area occupied per molecule from 100 to 0.2 nm^2 is interpreted as a gel-like structure at the surface. The presence of the surfactant seems to favor the formation of this interfacial structure. Finally, measurements of circular dichroism suggests a compaction of the protein due to the association with the surfactant given by an increase of α-helix structure in the complexes as compared to that of pure protein.* © 2006 Wiley Periodicals, Inc. Biopolymers 82: 261–271, 2006

Correspondence to: Félix Sarmiento; e-mail: fsarmi@usc.es

Contract grant sponsor: Spanish Ministerio de Educación y Ciencia, Plan Nacional de Investigación (I+D+i) (SMEC) and European Regional Development Fund (ERDF); contract grant number: MAT2005-02421 (SMEC).

*Permanent address: Grupo de Ciencia de Superficies y Coloides, Departamento de Química, Universidad Nacional del Sur, 8000 Bahía Blanca, Argentina.

This article was originally published online as an accepted preprint. The ''Published Online'' date corresponds to the preprint version. You can request a copy of the preprint by emailing the Biopolymers editorial office at biopolymers@wiley.com

Keywords: *human serum albumin; sodium perfluorooctanoate; surface characterization; pendant drop tensiometry; circular dichroism*

INTRODUCTION

Many biological systems with important commercial or technological importance contain mixtures of proteins and low molecular weight surfactants. Proteins in solution contain a mixture of different types of chemical groups (nonpolar, polar, and electrically charged) and hence it is not surprising that small amphiphilic molecules interact strongly with proteins. The chief driving force in the association of surfactant molecules into micelles and vesicles is the reduction in the hydrocarbon–water contact area of the alkyl chains.[1] Therefore, this same driving force may well favor the association of surfactant alkyl chains with hydrophobic parts of proteins molecules, while head groups of ionic surfactants will tend to interact attractively with positively charged groups on proteins. Both proteins and small molecule surfactants have a strong tendency to adsorb onto a wide range of hydrophilic and hydrophobic surfaces. In this manner, in systems containing a mixture of proteins and surfactant molecules, competitive adsorption between the two species occurs. Likewise, this competition will be strongly influenced by the nature and strength of the protein–surfactant interaction.[2] Specifically, the formation of protein–surfactant complexes in bulk solution reduces the amount of free surfactant available for competing with protein at the interface. In addition, any protein–surfactant binding may change the adsorption energy of the protein for the interface by affecting the net charge or the overall macromolecular hydrophobicity. There is a direct experimental link between studies of protein–surfactant binding and the competitive adsorption.[3]

Exceptional chemical and biological inertia and high gas-dissolving properties, excellent spreading characteristics, and high fluidity are the basis for the development of perfluorocarbons as a temporary oxygen carrier for use during surgery.[4] The adsorption and interfacial properties of protein–fluorocarbon surfactant mixtures are of particular interest in many biotechnological applications, such as the synthesis of blood substitutes.

The methods employed in detecting protein–surfactant interactions are often those of physical chemistry, which include optical,[5–7] hydrodynamic,[8] spectroscopic,[9–11] and radiactive[12] methods. Most of these approaches requires rather restrictive sample preparations[5–12]; therefore, it is difficult to measure the dynamic process of molecular interactions. Recently, a method based on surface tension measurements was developed for studying protein–surfactant interactions.[13] This method is based on the fact that molecular interactions will induce changes in the physicochemical properties, such as conformation of the protein. Because protein molecules are generally highly surface active, they easily adsorb at the surface and hence modify the surface properties, such as surface tension, of the protein solution.[14] Thus, measurements of surface tension will reflect the existence and nature of molecular interactions between proteins and surfactants. This method is flexible in its sample preparations and, more importantly, it is capable of conducting dynamic measurements and thus reveals dynamic aspects of molecular interactions. This latter feature is particularly useful as most biological processes are dynamic in nature.

Many techniques have been developed for surface tension measurements.[14–17] However, most of these techniques are restricted to static measurements and may have further limitations. For example, the Wilhelmy plate technique requires the establishment of a zero contact angle of the liquid at the plate; this is difficult to guarantee with systems involving proteins solutions because the protein readily adsorbs onto the plate and may render it hydrophobic.[18–20] Other surface tension measurement techniques, such as Du Noüy ring tensiometry, the drop volume technique or the maximum bubble method all lack of a suitable dynamic control.[14–17] In this sense, the pendant drop technique appears as the most appropriate experimental method. This technique is not only capable of producing highly accurate static surface tension results, but it is also being readily modified for dynamic surface tension measurements.[21–26] The pendant drop method relies on the shape of a drop as dictated by the classical Laplace equation of capillarity for surface tension determination. In this manner, the shape of the drop shape is identified by its characteristic dimensions such as the height and diameter[27] or a few preselected points such as the apex and inflection points along the drop profile.[28] A more versatile and

powerful approach, axisymmetric drop shape analysis (ADSA),[14,21–23] utilizes the entire drop profile, with equal importance attached to every profile point. With the advent of image analysis schemes, the drop profile may be obtained with subpixel resolution, leading to measurements with high degree of accuracy. ADSA has been applied to study the pressure,[29] temperature,[24] and time[24,30] dependence of interfacial tension, for both liquid–air and liquid–liquid systems. Dynamic surface tension can be measured under controlled conditions of surface perturbation. This may simulate many biological processes such as the surface dilation and compression of red blood cells[31–33] as well as mammalian lung.[34–38]

This work reports an interfacial characterization of human serum albumin (HSA)–sodium perfluorooctanoate (C8FONa) mixed solutions. First, the surface tension of the mixed system is analyzed and important structural information of the layer formed is extracted from these experiments. Second, the mixtures are characterized by circular dichroism spectroscopy to obtain further information on the denaturation process undertaken by the protein and the effect of the surfactant on this phenomenon.

EXPERIMENTAL

Materials

C8FONa was purchased from Lancaster Synthesis (97%). HSA (albumin $\geq$ 96%, essentially fatty acid free) was purchased from Sigma Chemical Co (St. Louis, Missouri, USA). It has a molecular weight of 66,000 Da. It is a carrier protein for fatty acid transport, free radical scavenging, and an osmotic regulator. It contains 585 amino acid residues and is 67% helical with no β-strands.[39] It has 17 disulfide bonds within three domains. Two of the domains contain binding sites for fatty acids and one is nonbinding. The single polypeptide contains internal hydrophobic ''pockets'' that house the hydrocarbon tails of the fatty acids and several different charged residues electrostatically binding the carboxylic ends. Albumin function for all transport stages is based on high conformation flexibility of the protein molecule and on the liability of its binding site characteristics. A comparison of the structure of liganded and unliganded HSA reveals dramatic conformational changes that occur when fatty acids bind. At pH $=$ 7 the size of such a HSA molecule is $14 \times 4 \times 4$ nm.[40]

Prior to the study it was verified that within the pH range of 5–8, HSA does not vary its three structural domains. Therefore, CF8ONa and HSA stock solution (1 mg/mL) were prepared by directly dissolving the appropriate amount of surfactant and protein in ultrapure water. Both solutions were kept in a refrigerator and diluted as required.

Langmuir Balance and ADSA

The experiments were performed with a constant pressure penetration Langmuir balance based on ADSA and described in detail elsewhere.[38] The whole setup, including the image capturing, the microinjector, the ADSA algorithm, and the fuzzy pressure control, is managed by a Windows integrated program (DINATEN). A solution droplet is formed at the tip of a coaxial double capillary, connected to a double microinjector. The program fits experimental drop profiles, extracted from digital drops micrographs, to the Young–Laplace equation of capillarity by using ADSA, and provides as outputs the drop volume V, the interfacial tension γ, and the surface area A. Area control uses a modulated fuzzy logic PID algorithm (proportional, integral, and derivative control) and is controlled by changing the drop volume in a controller manner. During the experiment, the drop is immersed in a glass tray (Hellma®) that is kept in a temperature-controlled cell by a Selecta thermostat bath with recycling water throughout all the experiments. The adsorption curves are measured by recording the change of interfacial tension at a constant interfacial area of 34 mm^2.

Surface Tension

Two types of mixed solutions were prepared: (1) HSA–C8FONa: 0.03 mg/mL HSA mixed with C8FONa (0.003–2 mg/mL); (2) C8FONa–HSA: 0.025 mg/mL C8FONa mixed with HSA (0.006–0.03 mg/mL). The dynamic surface tension of these solutions was recorded by means of the pendant drop tensiometer. Three days later, the experiment was repeated with the same solutions. Only for one specific HSA–C8FONa solution (0.03 mg/mL HSA + 0.018 mg/mL C8FONa) were the experiments repeated for 2–24 h intervals in those three days. All experiments were performed at (25 $\pm$ 0.01)°C.

Circular Dichroism (CD) Spectroscopy

A Jasco-715 automatic recording spectropolarimeter (Japan) was employed in the measurements of CD spectra, and a 0.2-cm path-length cell was used. CD spectra of pure HSA and HSA–C8FONa dilute solutions were recorded from 195 to 380 nm. The corresponding absorbance contribution of pure water was subtracted with the same instrumental parameters.

RESULTS AND DISCUSSION

Regimes of Dynamic Interfacial Tension

The properties of protein adsorption layers differ in many aspects from those characteristic of surfactants. At dilute concentrations, the dynamic interfacial tension can be divided into three time regimes for a pure protein solution. These are illustrated in Figure 1 for a 0.03 mg/mL HSA solution. In the beginning, the

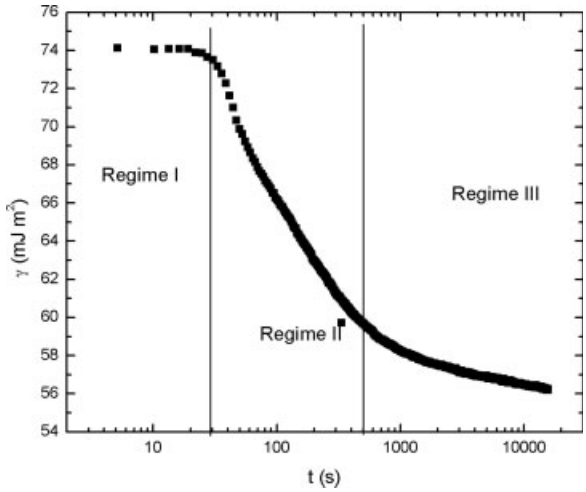

FIGURE 1 Adsorption regimes of pure HSA solution (0.03 mg/mL).

interfacial tension remains like that of the pure water and this regime is called the induction period. Regime II is characterized by a sharp decline in tension from this initial value. The final regime is a steady decline in interfacial tension, at a less negative slope than regime II on a semilog plot. Let us analyze in detail these three regimes encountered for a pure HSA solution and the manner in which they are respectively affected by the presence of perfluorocarbon in the solution. Figure 2 shows the dynamic interfacial variation of HSA–C8FONa mixture solutions vs. log t (t, time of adsorption).

Regime I: Induction Period. The first regime found in the interfacial tension experiments is an induction time in which the surface tension is that of the pure solution. This phenomenon has been previously observed in the adsorption of low-concentration proteins solutions at the air–water interface.[41–44] Some authors attributed this lag time to the tensiometry method used,[45,46] citing expansion of the surface due to initial protein adsorption and tension lowering for drop volume and pendant drop methods. Nevertheless, this is not valid in our case because the adsorption is recorded, maintaining the interfacial area constant along the experiment. Moreover, experiments employing static interfaces or the Wilhelmy plate methods have also noted a lag time, sometimes as longs as several hours.[42–47] Furthermore, radiotracer and ellipsometric techniques have indicated that the surface concentration does not exhibit this lag at early times.[42,47,48] Accordingly, at early times and low protein concentrations, molecules are present at the interface, but do not appreciably reduce the interfacial tension. Russev et al.[49] have reported a study, by ellipsometry, on the β-casein adsorption kinetics, where they observe the double layer formation. A dense protein layer initially forms, and then the adsorption continues in a second, more diffuse layer, which extends in the aqueous phase. Another interesting ellipsometric and surface pressure study[50] on the adsorption of this same protein supports the idea of a model that assumes the formation of a second layer adjacent to the primary adsorption layer. In the case of the pure HSA solution (0.03 mg/mL), the induction period lasts approximately 30 s, as can be seen in Figure 1. Let us observe the effect in the induction period caused by adding surfactant in the solution. It can be appreciated in Figure 2 how the presence of the surfactant has importantly modified the induction period shown. In particular, the lag time increases as the concentration of surfactant increases in the bulk until a certain C8FONa concentration is reached, and then it remains approximately constant. Specifically, 0.003, 0.012, and 0.021 mg/mL C8FONa added to the HAS provide an induction time of 60, 90, and 140 s, respectively, and the latter value is subsequently encountered for all further concentrations of C8FONa in the mixed solutions. From Figure 2 we also can see how the increase of surfactant concentration produces an abrupt decrease of the protein adsorption. As has been shown, an increase over five orders of magnitude on surfactant concentration becomes a 15–20% lower average molar area of the protein.[49] This means that the area occupied by molecules in the surface layer is several times lower,

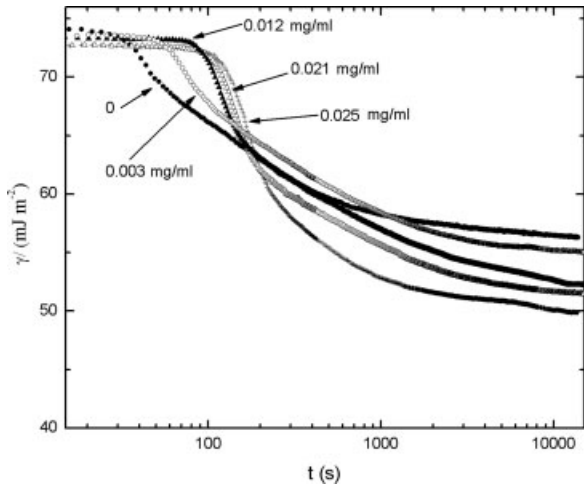

FIGURE 2 Variation of surface tension (γ) vs. log (t) for mixtures of 0.03 mg/mL HSA with C8FONa at different concentrations: (●) 0 mg/mL C8FONa; (○) 0.003 mg/mL C8FONa, (▲) 0.012 mg/mL C8FONa; (△) 0.021 mg/mL C8FONa, and (+) 0.025 mg/mL C8FONa.

which makes the competitive adsorption between protein and surfactant even more pronounced.

The induction period results from differences in the rate of adsorption onto the surface. The rate of arrival of molecules at the interface can be assumed as diffusion controlled.[51] For calculations of kinetics and dynamic surface tensions, the equation proposed by Ward and Todai[52] represents a general relationship between the dynamic adsorption and the surface $c(0, t)$ and reads for fresh and nondeformed surfaces,

$$\Gamma = 2\sqrt{\frac{D}{\pi}}\left[c_0\sqrt{t} - \int_0^{\sqrt{t}} c(0, t - t')d(\sqrt{t'})\right] \quad (1)$$

where c_0 is the protein bulk concentration, t is the time, and t' is a dummy integration variable. When the adsorption from solution takes place at a spherical surface (bubble or drop), the effect of surface curvature can be approximately accounted for by introducing an additional term into Eq. (1)[53,54]:

$$\Gamma = 2\sqrt{\frac{D}{\pi}}\left[c_0\sqrt{t} - \int_0^{\sqrt{t}} \mathrm{c}(0, t - t')d(\sqrt{t'})\right] \pm \frac{c_0 D}{r}t \quad (2)$$

where r is the radius of curvature, and a plus or minus sign before the second term on the right-hand side corresponds to a drop or bubble, respectively. Equation (2) can be simplified for very low concentrations (as the used in this work), and drop surfaces to[54]

$$\Gamma = 2c_0\sqrt{\frac{Dt}{\pi}} - \frac{c_0 Dt}{r} \quad (3)$$

For our calculations, we have assumed that the contribution of the second terms is on the order of experimental error. In this sense, some data have been reported.[54] We have assumed these simplifications because our fundamental interest is to have a visualization of the interfacial behavior of the protein, i.e., to facilitate the interpretation of experimental data of surface tension, Γ, which can be related to the surface pressure, Π, by the following equation:

$$\Pi(t) = RT[\Gamma(t)] \quad (4)$$

where $\Pi(t) = \gamma_0 - \gamma(t)$ and γ_0 is the interfacial tension of the pure fluids (in our case, water, $\gamma_0 = 72.8$ mJ/m^2). In this manner, one can calculate the diffusion coefficient of the different HSA–C8FONa mixture solutions from the slope of the $\Gamma(t)$ vs. $t^{1/2}$ dependence. The results are shown in Table I. For a typical protein, the diffusion coefficient is about 5×10^{-9} m^2/s.[41] The value obtained for pure HSA is somehow lower, $D_{HSA} = 1.93 \times 10^{-9}$ m^2/s. The value encountered for the mixed solutions decreases as the concentration of surfactant in solution increases. This feature completely agrees with the increasing values for the induction period shown in Figure 2 as the surfactant concentration increases. Therefore, a possible explanation of Table I shows the diffusion coefficient of the different HSA–C8FONa mixture solutions calculated from the slope of the $\Gamma(t)$ vs. $t^{1/2}$ graph. For a typical protein, the diffusion coefficient is about 5×10^{-9} m^2/s.[41] We found that $D_{HSA} = 1.93 \times 10^{-9}$ m^2/s; subsequently, the diffusion coefficient decreases as surfactant concentration increases. This observation suggests that surfactant molecules bind to the protein structure (a protein–surfactant complex can be formed) and causes conformational protein changes. The protein goes from a folded state (compact structure with hydrophobic groups at the protein interior) to an extended structure (unfolded). The extended protein state leads to a hydrophobic group exposition, which can interact with more surfactant molecules. As surfactant concentration augments, the molecules of such a compound available to interact with the HSA structure increases and a big complex could be formed. The complex size increases, reducing the rate of complex surface arrival and induction time augments. Besides, the structure of the protein might also change with association with the surfactants and this feature would similarly affect the interfacial behavior. Once a critical surface concentration of absorbed side chains is reached, the dynamic tension profile moves to regime II (Figures 1 and 2).

Regime II: Monolayer Saturation. Beyond a certain amount of adsorbed species, a steep decline in the interfacial tension is observed and continues for several seconds. As the interface becomes more saturated with protein, changes in both the surface concentration and interfacial tension are seen (Figure 2).

Table I Concentration of Sodium Perfluorooctanoate, *c*, Time of Adsorption, *t*, and Diffusion Coefficients, *D*, of the System Sodium Perfluorooctanoate + Human Serum Albumin

c (mg cm^{-3})	t (s)	D (m^2 s^{-1})
0	30	1.93×10^{-9}
0.003	60	1.50×10^{-9}
0.012	90	2.11×10^{-10}
0.021	140	2.32×10^{-11}
0.025	140	3.44×10^{-11}

Regime II appears very different, depending on surfactant concentration. In particular, as C8FONa concentration increases in the bulk solution, the decreasing slopes of the surface tension increase significantly and so does the final value. Once again, this feature provides information of the C8FONa–HSA complexes. Concretely, complexes formation occurs due to electrostatic interactions[55] and are more hydrophobic than the natural protein. Therefore, the surface activity of the complex is higher than that of the pure protein, resulting in a higher decrease of the surface tension. Accordingly, as the surfactant concentration increases in the solution, the complexes formed increase their activity, in agreement with the increasing slope found.

Regime III: Interfacial Gelation. The final regime is characterized by a slow decline in surface tension attributed to conformational changes of the adsorbed layer and by a continued building of a gel-like network. Adsorbed molecules in the initial layer continue changing their interfacial conformation in response to favorable environments for both hydrophobic and hydrophilic side chains. Subsequently, overlap and entanglement of these layers occurs, as the molecules seek more energetically favorable conformations. Multiple layers build into the water phase, as proteins aggregate and form branches. These branches connect at various points, and further aggregation is promoted as adsorbed HSA molecules slightly change conformation. The result is an amorphous gel-like network structure at the interface. The increasing interaction between molecules as the C8FONa concentration increases should be responsible for the lower surface tension values attained for the most concentrated solutions at longer times.

Surface Areas

To obtain structural information of the interfacial layer formed upon adsorption of mixed solutions, we can evaluate the dependence of Π on Γ by the following equation[47]:

$$\Pi(t) = RT[\Gamma(t)]^n \;\rightarrow\; \left\{\frac{1}{\Gamma(t)} = [a(t)]^n = \frac{RT}{\Pi(t)}\right\}, \tag{5}$$

where a is the surface area. When $n = 1$, the monolayer behaved like an ideal gas. Figure 3 represents the variation of log a vs. log t obtained in this manner for the mixed solutions. The curve form implies that $n > 1$ for these systems. In these curves, we can identify the adsorption regimes previously seen. Namely, regime I, the induction period, is characterized by diffusion of proteins to the interface and initiation of conformational changes of adsorbed protein molecules. Within this region, the number of molecules at the interface is very small, and consequently there are a small number of molecules at the interface, so that there is a great surface area available by molecule (the area occupied for a protein molecule at the interface is $\approx$100 nm^2). The HSA molecules at their native (folded) state are water soluble due to the presence of hydrophilic groups at the protein surface and did not migrate to the air–solution interface. Thus at early times and low protein concentration molecules are present at the interface but do not appreciably reduce the interfacial tension. This anomalous behavior extends to protein adsorption at the oil–water interface, which also exhibits an induction period in dynamic tension.[51] A strong adsorption arises from the presence of surface hydrophobic groups. When surfactant molecules interact with HSA, protein conformational changes occurs. The protein unfolding exposes the hydrophobic residues and makes the HSA molecules less water soluble, having to migrate to the air–water interface (to satisfy their amphiphilic behavior), so the adsorption increases. The dynamic tension profile moves to regime II. This feature happens similarly for pure HSA solutions and for HSA–C8FONa mixtures. At regime II, a strong adsorption arises from the presence of surface hydrophobic groups, and conformational changes occur. Unfolding of the proteins exposes new residues to the air phase, which also adsorb due to the similarities in environ-

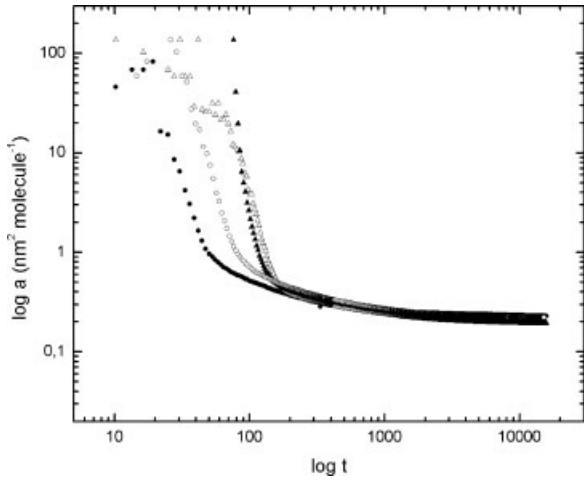

FIGURE 3 Surface area variations. Log (a) vs. log (t) for mixtures of 0.03 mg/mL HSA with C8FONa at different concentrations: (●) 0 mg/mL C8FONa; (□) 0.003 mg/mL C8FONa, (▲) 0.012 mg/mL C8FONa, and (△) 0.021 mg/mL C8FONa.

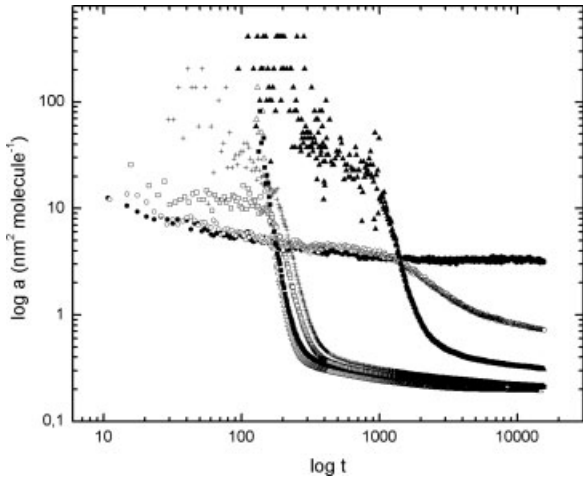

FIGURE 4 Surface area variations for mixtures of 0.025 mg/mL C8FONa with HSA at different concentrations: (●) 0 mg/mL HSA (○) 0.006 mg/mL HSA, (▲) 0.009 mg/mL HSA, (△) 0.012 mg/mL HSA, (■) 0.018 mg/mL HSA, (□) 0.025 mg/mL HAS, and (+) 0.03 mg/mL HSA.

ments of the nonpolar phase and interior of protein molecule. As a result, the surface area of the adsorbed molecule changes. Conformational changes of adsorbed HSA may provide a new environment for bulk proteins molecules that approach the initial adsorbed layer.

There is a drastic decline in the log a vs. log t curve (Figure 3), which represents the variation of surface area during conformational changes and increasing coverage of the interfacial layer. The interface progressively fills with protein molecules and HSA–C8FONA complexes that relax into less compact structures. Formation of multilayers may also be initiated. Figure 3 shows that the regime II decline in the log a vs. log t curve is more drastic as surfactant concentration increases. The hydrophobic interactions between surfactant tails and nonpolar protein residues that are newly exposed upon denaturation should increase and accelerate protein conformational changes.

Finally, at $t \approx 250$ s, there is a gradual fall in the surface area variation. That suggests initial gelation. In this regime, the conformational change of initially adsorbed layers continues. Multiple layers build into the water phase, as proteins aggregate and form branches. These structures form an amorphous network compact structure characterized by a surface area of about 0.2 nm^2/molecule. It is important to note that 0.2 nm^2/molecule is not the molecular area of HSA. It is the area occupied by molecule at the air–solution interface. In regime III, interfacial gelation, an amorphous gel-like network structure, was formed. Such a structure resulted from long-time molecular rearrangements, breakage, and formation of noncovalent structure-stabilizing bonds. The interaction between adjacent proteins produced lateral overlap and adsorbed layers entanglement. These facts contributed to surface pressure changes (and in consequence surface area changes) even when increases in the surface concentration ceased. As a result of these facts, a compact and dense structure was formed, where protein molecules were interconnected and overlapped. So the area occupied per molecule at the surface was very small because the air–solution coverage was elevated.

Figure 4 shows the variation of surface area logarithm vs. log t for different C8FONa–HSA mixtures. All the solutions have a fixed surfactant concentration (0.025 mg/mL) and variable HSA concentration. Two different sets of curves can be clearly appreciated in Figure 4. In the first three curves (HSA concentration of 0, 0.006, and 0.009), protein regimes become more evident as concentration increases. Nevertheless, there is probably not enough protein to form multilayers and gel-like structure at the surface. It is only above a certain protein concentration (0.012 mg/mL) that the three regimes appear and increasing HSA concentration provides hardly any more differences in the resulting surface area variation.

Figure 5 represents the variation of equilibrium surface area given by the value attained after 3 h of adsorption. It shows how a_{eq} decreases as [HSA] increases until a certain concentration (0.012 mg/mL), then it remains constant. This fact is in complete agreement with our above analysis. Before [HSA] = 0.012 mg/mL, there are not enough protein molecules to form a gel-like structure at equilibrium and the surface area values are higher.

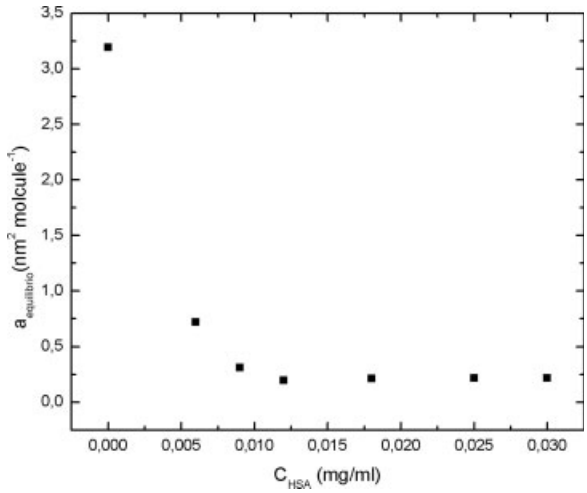

FIGURE 5 Equilibrium surface area (a_{eq}) vs. HSA concentration.

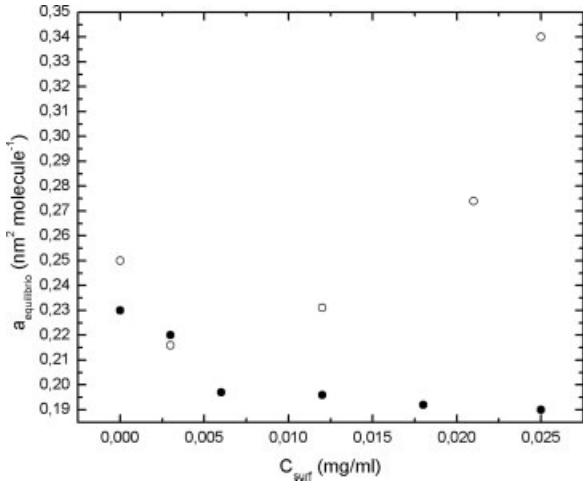

FIGURE 6 Equilibrium surface area (a_{eq}) vs. HSA concentration: (●) fresh solution and (○) three days later.

Time Effect: Extraction of Proteins from the Interface

Regarding the HSA, freshly prepared and three days later solutions provided hardly differences in the surface tension measurements. Figure 6 represents the a_{eq} variation vs. surfactant concentration calculated from measurements performed immediately and three days later. It can be seen how at the higher surfactant concentration the three-day solution shows a significant increase in the surface molecular area as compared to the fresh one in which the molecular area remains almost constant with increasing surfactant concentration. Accordingly, the interaction occurring between the protein and the surfactant molecules in the bulk solution seems to result in a certain increase of the area occupied per molecule once adsorbed at the interface. Hence, a longer time of interaction between the surfactant and the protein in the bulk might prevent the formation of an interfacial gel network.

To further evaluate the aging effect of surfactant molecules on HSA, we made surface tension measurements of the same solution (0.03 mg/mL HSA + 0.018 mg/mL C8FONa) on different days. The surface tension vs. log t and log a vs. log t curves are shown in Figures 7 and 8. It can be seen that the induction period increases with aging of the solution and the surface tension attained by aged mixed solutions decreases with its aging. Similar results that show a decrease in the surface activity of aged solutions were found recently for pure protein solutions.[56,57] The presence of the surfactant in the solution certainly seems to promote this lowering of the surface activity of the protein in two ways. First, the surfactant molecule competes with the protein adsorption, altering in this way the adsorption kinetics, as previously seen. Second, the γ increase is due to reduction of the HSA surface activity caused by their association with the surfactants. The effect is higher as the aging continues. Few studies have been found in the literature regarding the use of fluorinated surfactants for protein extraction. Among them, a lower protein solubilization potency was observed for compounds like tris(hydroxymethyl)aminomethane derived telomers: $C_nF_{2n+1}(CH_2)_2S[CH_2\ C(R)C(O)NHC(CH_2OH)_3]_pH$, with $n = 10$, $p = 4$.[58] Others studies indicate that ammonium perfluorooctanoate[59] is a potent solubilizing agent. The binding behavior is complex and involves a combination of electrostatic forces and hydrophobic interactions. Three distinct stages of protein–surfactant binding are proposed to occur. At early times, the surfactant binds to specific sites on the protein, in the case of C8FONa and HSA carboxilic head group and the 585 amino acid groups on HSA. This specific interaction with basic residues is stabilized by a hydrophobic interaction between the surfactant tails and adjacent sites on the protein surface. It does not significantly perturb the HSA conformation. Subsequently, the transitional binding regime occurs after all of the basic sites are occupied by specifically bound surfactants. Binding in this regime is evidently due to favorable hydrophobic interaction between fluorocarbon tails of C8FONa and possibly with hydrophobic protein surface domains, but it is noncooperative. Finally, there is a third regime, where there are cooperative bindings and which is associated with extensive conformational change. The main driving force is the hydrophobic interaction among surfactant tails with

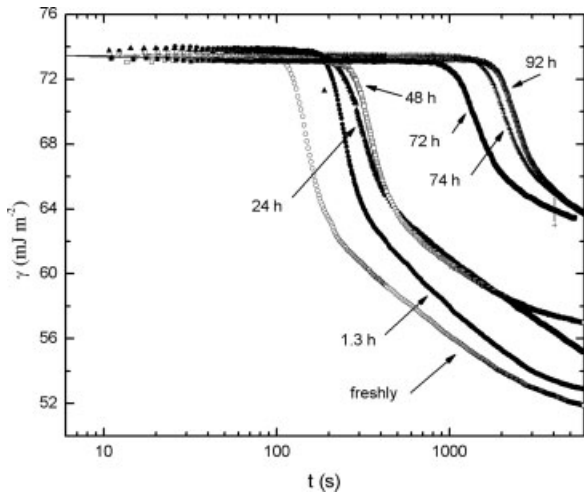

FIGURE 7 Time effect on surface tension variation vs. log (t) of a HSA–C8FONa mixture (0.03 mg/mL HSA + 0.018 mg/mL C8FONa): (○) fresh solution, (●) 1.3 later, (▲) 24 h later, (□) 48 hours later, (■) 72 h later, (△) 74 h later, and (+) 92 h later.

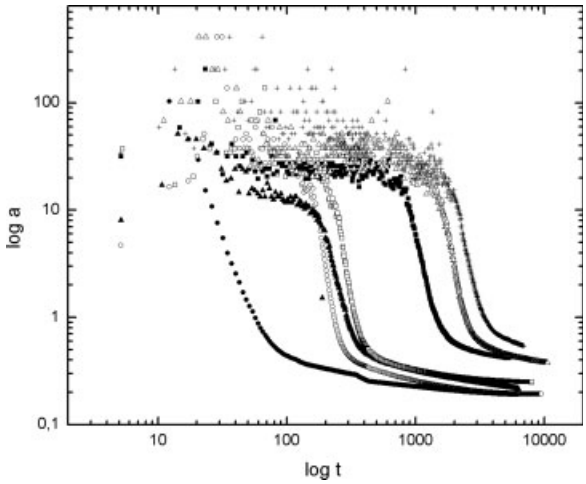

FIGURE 8 Log (a) vs. log (t) of a HSA–C8FONa mixture (0.03 mg/mL HSA + 0.018 mg/mL C8FONa): (●) fresh solution, (○) 1.3 h later, (▲) 24 h later, (□) 48 h later, (■) 72 h later, (□) 74 h later, and (+) 92 h later.

nonpolar proteins residues that are newly exposed upon denaturation. The protein eventually saturates with cooperatively bound surfactants. At this point, the complex resembles a protein solubilization. This last effect is appreciated only at the air–aqueous surface, and this feature was confirmed by CD measurements.

CD is an extraordinary sensitive technique to monitor the protein conformational change in the solution bulk. Figure 9 shows the molar ellipticity vs. wave length variation. The CD results were expressed in terms of mean residue ellipticity (MRE) in deg cm^2 $dmol^{-1}$, according the following equation[39]:

$$\text{MRE} = \frac{\text{Observed CD}(m\,\text{deg})}{C_\text{p} n l \times 10} \qquad (6)$$

where C_p is the molar concentration of the protein, n the number of amino acid residues (585), and l the path length (0.2 cm). The α-helical contents of free and combinated HSA were calculated from the MRE values at 208 nm using the following equation as described by Lu et al.[60]

$$\alpha\ \text{Helix}(\%) = \left[\frac{-\text{MRE}_{208} - 4000}{33,000 - 4000}\right] \times 100 \qquad (7)$$

where MRE_{208} is the observed MRE value at 208 nm, 4000 is the MRE of the β-form and random coil conformation cross at 208 nm, and 33,000 is the MRE value of a pure α-helix at 208 nm.

It can be seen in Figure 9 that the native HSA solution (0.03 mg/mL) has a 42.25% of α-helix, while all HSA–C8FONa dilute solutions have an α-helix average of 52.23%. Therefore, there is a cooperative effect between HSA and C8FONa molecules. The presence of surfactant molecules stabilized protein structures and increased it ellipticity, producing the same effect as the aggregate of a buffer solution (α-helix % = 51). It can be seen that the (α-helix) amount increases and thus the protein becomes more compact upon association with the surfactant. In dilute solutions, the majority of HSA and surfactant molecules are located at the surface and it is there where the conformational changes and denaturation occurs. Although the occurrence of extensive protein conformations change in this regime is more or less understood, the structure of the resulting complexes is an extremely interesting questions that remains unclear.

CONCLUSIONS

In this research, the dynamics of adsorption of a set of different C8FONa–HSA solutions has been examined in detail. First, pendant drop tensiometry shows the different regimes undergone by the interfacial layer as it increases its coverage by analysis of the evolution of the surface tension with time for a pure HSA solution at a certain concentration. Initial protein adsorption is favored by the hydrophobic interactions occurring between the air phase and the hydrophobic segments of the protein. The formation of C8FONa–HSA complexes in the bulk solution seems to increase the hydrophobicity of the molecule with respect to that of pure protein. Accordingly, an

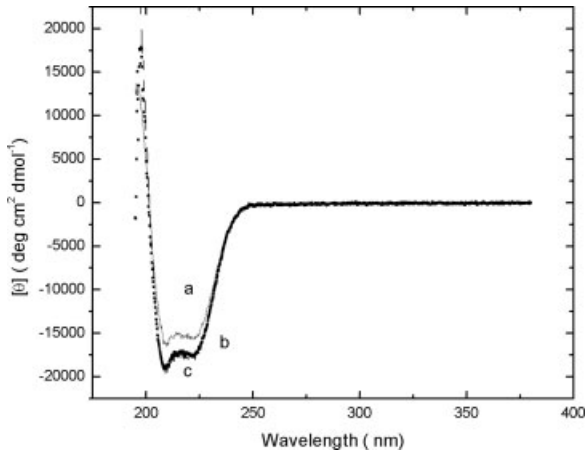

FIGURE 9 CD spectrum. MRE (mean residue ellipticity) vs. wavelength: (a) HSA native solution (2 μM), (b) 2 μM HSA + 10 mM (100 mM Na_2HPO_4/1M NaCl), (c) 2 μM HSA +1.4 mM C8FONa.

increase in the surface activity was found in the dynamic surface tension curves. Specifically, the initial adsorption layer provided a basis for the further adsorption and even interfacial aggregation of molecules. Moreover, large strands of aggregates proteins seem to appear at large periods of time. In addition, differences in the values of the induction period appeared in the dynamic surface tension curves obtained for the mixtures—namely, the lag time increases with increasing concentration of surfactant. To shed light on this matter, the diffusion coefficients of the pure protein solution, as well as of the mixed solution, were calculated. The values obtained in this manner agree with those found in the literature and provide evidence of a higher induction period due to a decrease of the diffusion coefficient of the mixtures with respect to that of the pure protein. In addition, the existence of different adsorption regimes has been evaluated by analysis of the surface area variation with time. A gel structure formation can be inferred from these results and in which an area reduction from 100 to 0.2 nm^2 per molecule is shown. Furthermore, the presence of the surfactant in the solution seemed to favor this gel structure in view of the even higher area per molecule encountered. Finally, the effect of aging of the pure protein solution as well as of the mixture has been carefully studied to further understand the interaction taking place between C8FONa and HSA. The evolution of the surface tension of the mixed solution has been measured again at subsequent periods of time going from one hour to three days. A reduction of the surface activity of the protein as well as of the mixtures was found. This feature is interpreted in terms of the interaction between protein and surfactant and as a conclusion: the C8FONa seems to solubilize the protein, increasing their hydrophobic character. Moreover, the main driving force encountered is the hydrophobic interaction between surfactant tails and nonpolar protein residues that are newly exposed upon denaturation.

The authors acknowledge the financial support from Spanish Ministerio de Educación y Ciencia, Plan Nacional de Investigación (I+D+i), MAT2005-02421 and by the European Regional Development Fund (ERDF). PM thanks Fundación Antorchas, Argentina (project 4308-110), for her grant.

REFERENCES

1. Israelachvili, J. N. Intermolecular and Surface forces with Application to Colloidal and Biological Systems; Academic Press: London, 1985.
2. Dickinson, E.; Euston, S. R.; Woskett, C. M. Prog Colloid Polym Sci 1990, 82, 65–75.
3. Cockbain, E. G. Trans Faraday Soc 1953, 49, 104–111.
4. Riess, J. G. In Blood Substitutes: Principles, Methods, Products and Clinical Trials; Chang, T. M. S., Ed.; Karger Publishers: New York, 1998; Vol 2, p 101.
5. Anderson, S. R.; Weber, G. Biochemistry 1969, 8(1), 371–377.
6. Slayter, E. M. J Mol Biol 1965, 14(2), 443–452.
7. McClure, R. J.; Craven, B. M. J Mol Biol 1974, 83(4), 551–554.
8. Bloomfield, V. Biochemistry 1966, 5(2), 684–689.
9. Parks, J. S.; Cistola, D. P.; Small, D. M.; Hamilton, J. A. J Biol Chem 1983, 258(15), 9262–9269.
10. Sklar, L. A.; Hudson, B. S.; Simoni, R. D. Biochemistry 1977, 16(23), 5100–5108.
11. Housainndokht, M. R.; Jones, M. N.; Newall, J. F.; Prieto, G.; Sarmiento, F. J Chem Soc Faraday Trans 1993, 89(12), 1963–1968.
12. Spector, A. A.; John, K.; Fletcher, J. E. J Lipid Res 1969, 10(1), 56–67.
13. Chen, P.; Policova, Z.; Susnar, S. S.; Pace-Asciak, C. R.; Demin, P. M.; Neumann, A. W. Colloid Surf A 1996, 114, 99–111.
14. Neumann, A. W.; Spelt, J. K. Eds.; Applied Surface Thermodynamics; Dekker: New York, 1996.
15. Robb, I. D. In Surfactant Science Series, Vol 11, Anionic Surfactants; Lucassen-Reyndess, E. H., Ed.; Dekker: New York, 1981.
16. Gaines, G. L., Jr. Insoluble Monolayers at Liquid-Gas Interfaces; Wiley—Interscience: New York, 1966.
17. Adamson, A. W. The Physical Chemistry of Surfaces, 5th ed.; Wiley: New York, 1990.
18. Chen, P.; Lahooti, S.; Policova, Z.; Cabrerizo-Vílchez, M. A.; Neumann, A. W. Colloids Surf B 1996, 6(4–5), 279–289.
19. Miller, R.; Treppo, S.; Voigt, A.; Zingg, W.; Neumann, A. W. Colloids Surf 1993, 69(4), 203–208.
20. Chen, P.; Kwok, D. Y.; Prokop, R. M.; del Rio, O. I.; Susnar, S. S.; Neumann, A. W. In Drops and Bubbles in Interfacial Research; Möbius, D., Miller, R., Eds.; Elsevier: Amsterdam, 1977; Chap 2.
21. Rotenberg, Y.; Boruvka, L.; Neumann, A. W. J. Colloid Interface Sci 1983, 93(1), 169–183.
22. Chen, P.; Li, D.; Boruvka, L.; Rotenberg, Y.; Neumann, A. W. Colloids Surf 1990, 43(2–4), 151–167.
23. Chen, P.; Neumann, A. W. Colloids Surf 1992, 62(4), 297–305.
24. Cabrerizo-Vilchez, M. A.; Policova, Z.; Kwok, D. Y.; Chen, P; Neumann, A. W. Colloids Surf B 1995, 5(1–2), 1–9.
25. Jyoti, A.; Prokop, R. M.; Neumann, A. W. Colloids Surf B 1997, 8(3), 115–124.
26. Prokop, R. M.; Jyoti, A.; Eslamian, M.; Garg, A.; Mihaila, M.; del Rio, O. I.; Susnar, S. S.; Policova, Z.; Neumann, A. W. Colloids Surf A 1998, 131(1–3), 231–247.
27. Girault, H. H. J.; Schiffrin, D. J.; Smith, B. D. V. J. Colloid Interface Sci 1984, 101(1), 257–266.

28. Maze, C.; Burnet, G. Surface Sci 1971, 24(1), 335–342.
29. Susnar, S. S.; Hamza, H. A.; Neumann, A. W. Colloids Surf A 1994, 89(2–3), 169–180.
30. Voigt, A.; Thiel, O.; Williams, D.; Policova, Z.; Zingg, W.; Neumann, A. W. Colloids Surf 1991, 58(3), 315–326.
31. Zhong-can, O.-Y.; Helfrich, W. Phys Rev Lett 1987, 59(21), 2486–2488.
32. Helfrich, W. Z Naturfors C 1973, 28(11–12), 693–703.
33. Helfrich, W. Z Naturfors C 1974, 29(9–10), 510–515.
34. Notter, R. H.; Finkelstein, J. N. J Appl Physiol Respir Exerc Physiol 1984, 57(6), 1613–1624.
35. Goerke, J.; Clements, J. A. In Handbook of Physiology; Macklem, P. T., Mead, J., Eds.; American Physiological Society: Bethesda, MD, 1986; Chap 16, Sec 3, p 247.
36. Schürch, S. Clin Perinatol 1993, 20(4), 669–682.
37. Scarpelli, E. M. Surfactants and the Living of the Lung; John Hopkins University Press: Baltimore, MD, 1988.
38. Cabrerizo-Vílchez, M. A.; Wege, H. A.; Holgado-Terriza, J. A. J A Rev Sci Instrum 1999, 70(5), 2438–2444.
39. Dockal, M.; Carter, D. C.; Rüker, F. J Biol Chem 2000, 275, 3042–3099.
40. Peters, T. Adv Protein Chem 1985, 37, 161–245.
41. Graham, D. E.; Phillips, M. C. J Colloid Interface Sci 1979, 70(3), 415–426.
42. Benjamins, J.; de Feijter, J. A.; Evans, M. T. A. Graham, D. E.; Phillips, M. C. Faraday Discuss Chem Soc 1975, 59, 218–229.
43. Song, K. B.; Damodaran, S. Langmuir 1991 7(11), 2737–2742.
44. Ivanova, M.; Verger, R.; Bois, A. G.; Panaiotov, I. Colloids Surf 1991 54(3–4), 279–296.
45. Ward, A. J. I.; Regan, L. H. J Colloid Interface Sci 1978, 66(1), 195–196.
46. Tornberg, E. J Colloid Interface Sci 1978, 64(3), 391–402.
47. Graham, D. E.; Phillips, M. C. J Colloid Interface Sci 1979, 70(3), 403–414.
48. Morrissey, B. W.; Han, C. C. J Colloid Interface Sci 1978, 65(3), 423–431.
49. Russev, S. C.; Arguirov, T., VI; Gurkov, T. D. Colloids Surf B 2000, 19(1), 89–100.
50. Grigoriev, D. O.; Fainerman, V. B.; Makievski, A. V.; Krägel, J.; Wüstneck, R.; Miller, R. J Colloid Interface Sci 2002, 253(2), 257–264.
51. Beverung, C. J.; Radke, C. J.; Blanch, H. W. Biophys Chem 1999, 81(1), 59–80.
52. Ward, A. F. H.; Tordai, L. J Chem Phys 1946, 14(7), 453–461.
53. Liggieri, L.; Ravera, F.; Ferrari, M.; Passerone, A.; Miller, R. J Colloid Interface Sci 1997, 186(1), 46–52.
54. Makievski, A. V.; Loglio, G.; Krägel, J.; Miller, R.; Fainerman, V. B.; Neumann, A. W. J Phys Chem B 1999, 103(44), 9557–9561.
55. Miller, R.; Fainerman, V. B.; Aksenenko, E. V.; Leser, M. E.; Michel, M. Langmuir 2004, 20(3), 771–777.
56. Fainerman, V. B.; Zholob, S. A.; Leser, M.; Michel, M.; Miller, R. J Colloid Interface Sci 2004, 274(2), 496–501.
57. Miller, R.; Fainerman, V. B.; Makievski, A. V.; Krägel, J.; Grigoriev, D. O.; Kazakov, V. N.; Sinyachenko, O. V. Adv Colloid Interface Sci 2000, 86(1–2), 39–82.
58. Maurizis, J. C.; Pavia, A. A.; Pucci, B. Bioorg Med Chem Lett 1993, 3(2), 161–164.
59. Shepherd, F. H.; Holzenburg, A. Anal Biochem 1995, 224(1), 21–27.
60. Lu, Z. X.; Cui, T.; Shi, Q. L. Application of Circular Dichroism and Optical Rotatory Dispersion in Molecular Biology; Science Press: Peking, 1987.

Reviewing Editor: Laurence Nafie